Calligraphic poling of Lithium Niobate

Makan Mohageg, Dmitry V. Strekalov, Anatoliy A. Savchenkov, Andrey B. Matsko, Vladimir S. Ilchenko and Lute Maleki

Jet Propulsion Lab, Quantum Sciences and Technology Group, California Institute of Technology, Pasadena, CA 91109
makan.mohageg@jpl.nasa.gov

Abstract: We demonstrate a novel technique for instituting complex and arbitrary shaped micron-scale domain patterns in $LiNbO_3$ at room temperature. Fabrication of continuous domains as narrow as 2 μm across and hexagonal patterns of the same order accompanied by real time visualization of the poling process are presented.

OCIS codes: (160.2260) Ferroelectrics; (190.4360) Nonlinear optics, devices

References and Links

1. G.A. Magel, M.M. Fejer, R.L. Byer "Quasi-phase-matched second-harmonic generation of blue light in periodically poled $LiNbO_3$," Appl. Phys. Lett. **56**, 108 — 110 (1990)
2. L.E. Myres, R.C. Eckardt, M.M> Fejer, R.L. Byre, W.R. Bosenberg, J.W. Pierce, "Quasi-phase matched optical parametric oscillators in bulk periodically poled $LiNbO_3$," J. Opt .Soc. Am. B **12**, 2102 — 2116 (1995)
3. M. Houé, P.D. Townsend, "An introduction to methods of periodic poling for second harmonic generation," J. of Phys. D: Appl. Phys **28**, 1747 — 1763 (1995)
4. M. Yamada, "Elelctrically induced Bragg-diffraction grating composed of periodically inverted domains in lithium niobate crystals and its application devices," Rev. of Sci. Instr. **71**, 4010 — 4016 (2000)
5. E.J. Lim, M.M. Fejer, F.L. Byer, W.J. Kozlovsky, "Blue light generation by frequency doubling in periodically poled lithium niobate channel waveguide," Electron. Lett. **25**, Issue 11, 731 –- 732 (1989)
6. M.M. Fejer, G.A. Magel, D.H. Jundt, R.L. Byer, "Quasi-Phase-Matched Second Harmonic generation: Tuning and tolerances," IEEE J. Quantum Electron. **28**, No. 11, 2631 –- 2654 (1992)
7. N.G.R. Broderick, G.W. Ross, H.L. Offerhaus, D.J. Richardson, D.C. Hanna, "Hexagonally poled lithium niobate: A two dimensional nonlinear photonic crystal," Phys. Rev. Lett. **84**, No. 19, 4345 –- 4384 (2000)
8. K.S. Zhang, T. Coudreau, M. Martinelli, A. Maitre, C. Fabre, "Generation of bright squeezed light at 10.6 μm using cascaded nonlinearities in a triply resonant cw periodically poled lithium niobate optical parametric oscillator," Phys. Rev. A **64** (2001)
9. M. Yamada, N. Nada, M. Saitoh, K. Watanabe, "First order quasi-phase matched $LiNbO_3$ waveguide periodically poled by applying an external field for efficient blue second harmonic generation," Appl. Phys. Lett. **62**, 435 – 436 (1992)
10. R.G. Batchko, V.Y. Shur, M.M. Fejer, R.L. Byer, "Backswitch poling in lithium niobate for high-fidelity domain patterning and efficient blue light generation," Appl. Phys. Lett. **75**, 1673 – 1675 (1999)
11. V.Y. Shur, E.L. Rumyantsev, E.V. Nikolaeva, E.I. Shishkin, E.V. Fursov, R.G. Batchko, L.A. Eyres, M.M. Fejer, R.L. Byer, "Nanoscale backswitched domain patterning in lithium niobate," Appl. Phys. Lett. **76**, 143 – 145 (2000)
12. V.S. Ilchenko, A.A. Savchenkov, A.B. Matsko, L. Maleko, "Nonlinear Optics and Crystalline Whispering Gallery Mode Cavities," Phys. Rev. Lett. **92**, No. 4043903 (2004)
13. H.A. Eggert, B. Hecking, K. Buse, "Electrical fixing in near-stoichiometric lithium niobate crystals," Opt. Lett. **29**, No. 21, 2476 – 2478 (2004)
14. K. Terabe, M. Nakamura, S. Takekawa, K. Kitamura, S. Higuchi, Y. Gotoh, Y. Cho, "Microscale to nanoscale ferroelectric domain and surface engineering of a near-stoichiometric $LiNbO_3$ crystal," Appl. Phys. Lett. **82**, No. 3, 433 – 435 (2003)
15. G. Rosenman, P. Urenski, A. Agronin, Y. Rosenwaks, M. Molotskii, "Submicron ferroelectric domain structures tailored by high voltage scanning probe microscopy," Appl. Phys. Lett **82**, No. 1, 103 – 105 (2003)
16. B.J. Rodriquez, R.J. Nemanich, A. Kingon, A. Gruverman, S.V. Kalinin, K. Terabe, X.Y. Liu, K. Kitamura, "Domain growth kinetics in lithium niobate signel crystals studied by piezoresponse force microscopy," Appl. Phys. Lett. **86**, 012906 (2005)
17. Y. Cho, K. Fujimoto, Y. Hiranaga, Y. Wagatsuma, A. Onoe, K. Terabe, K. Kitamura, "Tbit/inch^2 ferroelectric data storage based on scanning nonlinear dielectric microscopy," Appl. Phys. Lett. **81**, No. 23, 4401 – 4403 (2002)
18. K. Fujimoto, Y. Cho, "High-speed switching of nanoscale ferroelectric domains in congruent single-crystal $LiTaO_3$," Appl. Phys. Lett. **83**, 5265 – 5267 (2003)

19. S. De Nicola, P. Ferraro, A. Finizo, S. Grilli, G. Coppola, M. Iodice, P. De Natale, M. Chiarini, "Surface topography of microstructures in lithium niobate by digital holographic microscopy," Meas. Sci. Tech. **15**, 961 – 968 (2004)
20. V.S. Ilchenko, A.B. Matsko, A.A. Savchenkov, L. Maleki, "Low threshold parametric nonlinear optics with quasi-phase-matched whispering-gallery modes," J. Opt .Soc. Am. B **20**, No. 6, 1304 – 1308 (2003)
21. M. Mohageg, A.B. Matsko, A.A. Savchenkov, D. Strekalov, V.S. Ilchenko, L. Maleki, "Reconfigurable Optical Filter," Electron. Lett. **41**, 356-358 (2005)
22. H. Ishizuki, T. Taira, S. Kurimura, J.H. Ro, M. Cha, "Periodic poling in 3-mm-thick MgO:$LiNbO_3$ Crystals," Japanese J. of Appl. Phys. **42**, 108 – 110 (2003)
23. M. Müller, E. Soergal, K. Buse, "Visualization of ferroelectric domains with coherent light," Opt. Lett. **28**, 2515 – 2517 (2003)
24. D.H. Jundt, "Temperature-dependant Sellmeier equation for the index of refraction, n_e, in congruent lithium niobate," Opt. Lett. **22**, 1553 – 1555 (1997)

1. Introduction

Constructing periodically poled $LiNbO_3$ (PPLN) structures is of great importance in nonlinear optics and quantum optics. Optical parametric oscillators [1-3], Bragg reflectors [4], second harmonic generators [5,6], photonic bandgap devices [7], and the generators of squeezed light [8] have all been demonstrated with PPLN.

Poling $LiNbO_3$ causes a localized reversal in the direction of the permanent polarization of the crystal. Techniques involving wet etching and photolithographic preformed masks [9-11] have generally been used for poling purposes. These methods, while readily applicable to multiplicative reproducing of simple domain patterns, such as linear gratings, are not convenient for the real time generation and visualization of patterns of arbitrary shapes, as required in some fundamental applications [12], because the techniques require the fabrication of a photolithographic mask each time the domain map changes.

Recently, domain structures in $LiNbO_3$ crystals formed through an 'electrical fixing' technique have been reported [13]. In this experiment, an electric bias field interacted with an optical hologram within bulk $LiNbO_3$ to cause domain reversal in the region defined by the hologram. With this method, the complexity of given domain structures are limited by the availability and quality of optical holograms.

A new technique to pole thin $LiNbO_3$ crystals while monitoring the growth of domain walls *in situ* has been developed and is presented in this paper. This technique is called *calligraphic poling,* because rather than charging a preformed mask, a micron sized electrode that drags charge across the surface of the crystal causes domain reversal in real time. The shape of the resulting reversed domain is then given by the electrode trajectory with breaks in the poling structure introduced by switching the voltage off as desired.

There are advantages of calligraphic poling when compared to traditional approaches. This method is flexible and allows generating an arbitrary complex domain pattern on a crystal without the fabrication of an expensive mask. The poling process can be optically observed and manipulated in real time. This method does not require extreme environment conditions; all calligraphic poling experiments discussed in this paper were conducted with a table top setup at room temperature and at atmospheric pressure. Domain reversal occurs fast enough to make calligraphic poling practical for measuring domain wall growth and domain flipping dynamics in general. In fact, for small wafers this technique can be not only more versatile but also faster than conventional ones. This aspect is very important for research labs.

Calligraphic poling is similar in nature and motivation, although different in implementation and execution, to the growing field of poling ferroelectric crystals with scanning force microscopes (SFM). In SFM poling experiments, actual SFMs were used to generate nm scale domain structures on either crystal samples that were not thicker than 1 μm with bias fields of tens of volts [14], or crystal samples several hundred micrometers thick with bias fields of over 3 kV [15]. Calligraphic poling uses only the tip of the SFM probe to generate domains structures that are generally tens of micrometers in size in crystals that are up to 250 μm thick. Because of the focus on micrometer sized domains, the domain flipping

process is visualized in real time with calligraphic poling. Nanometer-scale SFM poling structures are to be visualized after the poling process has completed.

We demonstrate complex domain structures with two types of poling patterns: curves and hexagons. Curves are fabricated when a micron thick needle electrode moves across the crystalline wafer, while the hexagons are generated when the tip of the electrode is stationary. Narrow domains less than 2 μm across are fabricated either as straight, smooth lines or as curves across the single-domain crystal.

Changes to the poling process due to alignment of the narrow tungsten electrode with the crystal **x** and **y** axes have not been observed. Domains in the shape of hexagons (as determined by the crystal structure of $LiNbO_3$) are readily obtained. Hexagon poling is interesting because it allows for studies of crystal purity. We have observed symmetric hexagon generation in stoichiometric material and asymmetric hexagon generation in congruent material. Hexagonally poled $LiNbO_3$ could be used to create photonic bandgap devices at visible wavelengths. In previous implementations of hexagon poling, an array of hexagons was lithographically applied to a mask, which then had to be aligned to the crystal axes [7]. With calligraphic poling, the alignment of the "naturally grown" hexagons is automatic.

We verified our technique for congruent crystals that are less than 200 μm thick and stoichiometric crystals less than 250 μm thick. Thicker crystals require larger poling voltages than we have access to. We found that inhomogeneities in crystal composition play a decidedly large role in the poling process. Both the domain growth rate and the minimum poling voltage depend on location on the crystal surface where the tip electrode is applied. Hence, our setup can be used for nondestructive tests of the crystal purity. It is possible to study wafer structure by making a domain pattern over it. After the testing, the domain pattern can be easily removed.

2. Calligraphic poling

2.1 Instrumentation

The calligraphic poling machine consists of a sharp edged tungsten electrode (the pen, or the sharp electrode) that brushes across the surface of the crystal, a flat polished electrode, and a translation stage to change the position of the sharp electrode with respect to the crystal. By applying a voltage between the pen and the substrate, domain structures are drawn directly onto the crystal in a user defined pattern. A diagram of the calligraphic poling machine is shown in Fig. 1.

The sharp electrodes are the same as probes in atomic force microscopy. We found that pen electrodes made of a solid shank of tungsten are better suited for calligraphic poling than bent electrodes with 'cat-whisker' tungsten tips, cut copper wire, or the edge of a razor. Since the pen is in physical contact with the upper surface of the crystal, excessive pressure applied may cause either the crystal or the pen to break. Using a razor will usually cause a crack to form in the crystal, while the whisker-like tip will certainly bend and break under even modest strain. Using the crimped end of a piece of copper wire is an attractive choice for engineering narrow domain structures. However, the lack of rigidity in copper wires allows for hysterisis in motion and uncontrollable slipping when this sort of pen is moved.

Choosing the appropriate solid tungsten probe is critical. It was found that pen electrodes of 1 μm radius work best. Larger radius pen electrodes automatically exclude straightforward engineering of small domains. Smaller radius pen electrodes initially allow for smaller domain structures. However, after some time, the stress of dragging the pen across the surface of the crystal will cause the pen electrode to bend. Charge build up will cause domain flipping to occur along the position of the bend in the electrode instead of at the tip of the electrode.

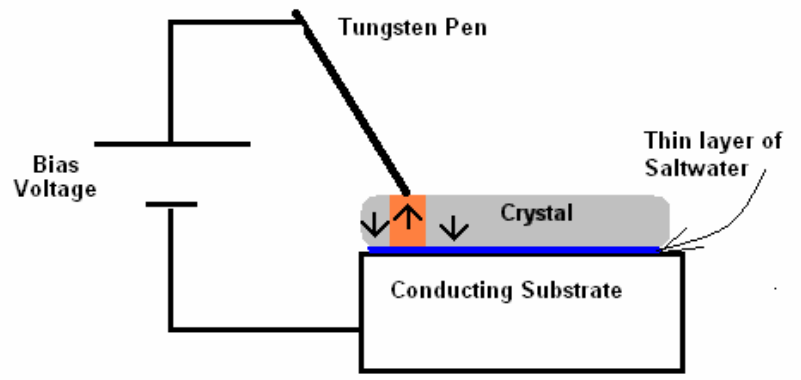

Fig. 1. A diagram of the calligraphic poling machine. The tungsten pen is free to move across the surface of the crystal. When voltage is applied, domain reversal takes place locally under the position of the pen. The arrows represent the direction of the polarization for local regions on the crystal.

Minimizing the mechanical stress applied by the pen to the crystal is important for calligraphic poling to give reproducible results. In Fig. 1, the pen is deliberately depicted as making an angle with the surface of the crystal. The pen is connected to the voltage source by a mount which allows a small amount of rotation in the plane perpendicular to the crystal surface and parallel to the projection of the pen onto the crystal surface. Thus, as the pen is placed into contact with the crystal, rather than applying stress to the crystal, the angle made between the direction of the pen and the vector that is normal to the surface of the crystal will increase to keep the applied stress near zero. If the initial angle is too small or if the pen mounting is too firm, the crystal (or pen) will crack as described above.

For a nearly flat crystal, the angle made between the normal and the pen stays roughly constant at all points on the surface. By controlling this angle, the size of the generated domain structures can be controlled. We have observed that a small angle yields small domain structures, while a large angle yields larger domain structures. In the context of generating large, smooth curve-like domain structures with calligraphic poling, increasing the angle the pen makes with the normal vector of the crystal surface is preferable to increasing the bias field.

Fixing the pen so that it is unable to rotate will enable studies of domain flipping dynamics while the crystal is under stress or strain. However, applying too much stress unevenly throughout the crystal may cause the crystal to form a crack. Further, when a liquid electrode is used, we found that applying stress to the crystal may cause dry regions to form in the areas between the substrate and the bottom of the crystal. This will change the poling dynamic significantly. With all this in mind, there is still an opportunity to observe how ferroelectric flipping dynamics change under mechanical stress of small magnitude.

The lower surface of the crystal is placed into contact with a polished flat electrode (the substrate). A thin layer of salt water is placed between the substrate and the crystal to ensure uniform electrical contact between the two nearly-flat surfaces. Furthermore, a thin layer of salt water serves as a strong binding agent between the crystal and the substrate.

Two different materials were successfully used as the substrate. The thin plate of a metallic mirror was initially chosen because of its excellent surface quality. However, sparks can cause cracks to form on the thin metal surface which may electrically isolate different parts of the substrate surface. Because of this recurring issue, a solid piece of brass with one polished surface was used as the substrate instead of the metallic mirror. Scratches and cracks along the surface do not result in electrical isolation because of the thickness of the substrate and the salt water coating. However, surface defects deeper than several dozen microns can

collect dust particles and other contaminants which cause sparking at a lower voltage than that which is required for domain reversal.

2.2 Dynamics

The size and shape of the produced domains is controlled by the magnitude of the voltage bias between the pen and the substrate, as well as the duration of the applied voltage. For a typical crystal specimen that is 100 µm thick along the z-axis and cut into a cylinder of radius 5 mm, voltages from 2—3 kV applied over time periods less than 2 s to a motionless pen yield hexagons; while intermediate voltages (800 V—1.8kV) applied over longer time periods to a moving pen yield straight lines and curves. Crystal thickness also affects the poling dynamic. We observed that the resultant domains in a thick crystal are smaller than those of a thin crystal when applied to the same voltage for the same amount of time. Figure 2 and Fig. 3 show some typical results achieved with the poling process.

Stoichiometric crystals, that is, crystals that have a ratio of Li to Nb that is near unity, show domain reversal at much lower voltages—typically at or around 400 V for a crystal of the same thickness described above. Poling stoichiometric crystals results almost exclusively in uniform hexagonal shaped domain patterns.

As the temperature of a ferroelectric approaches its Curie temperature, the bias field for causing domain reversal will decrease significantly. The Curie temperature of $LiNbO_3$ is well over 1400º C. To approach this value and realize the benefits of poling at high temperatures will require additional instrumentation and a redesign of the calligraphic poling machine.

Note that the values for required voltages reported in this article for both congruent and stoichiometric material follow similar relationships to those described in SFM poling experiments [16].

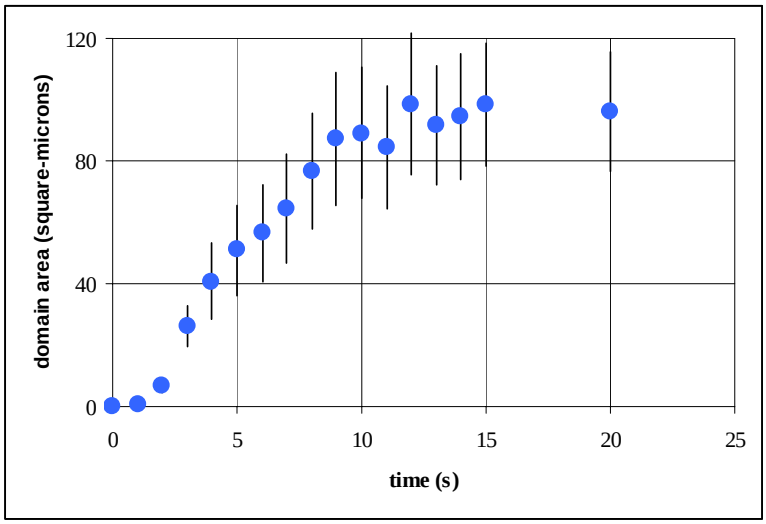

Fig. 2. Poling dynamics of a 200 µm thick specimen of congruent $LiNbO_3$. 3 kV of bias was applied through a 1 µm tungsten pen and the surface area of the resultant domain structure was recorded. This experiment was repeated nine times at various locations on the crystal to obtain the error bars.

The poling dynamics for congruent and stoichiometric $LiNbO_3$ through calligraphic poling are different. It has been observed elsewhere that the required bias fields for domain reversal in stoichiometric $LiNbO_3$ is a fraction of the bias field required for domain reversal in congruent $LiNbO_3$. Measurements of the size of domains generated by calligraphic poling as a function of bias voltage exhibit the same general dependence.

Figure 2 shows dynamics data for poling congruent $LiNbO_3$. Figure 3 shows the same type of data for stoichiometric $LiNbO_3$. Each data point is an average of 5 points taken with the same parameters on different regions of the same crystal to average out any differences in structural content of the crystal. The crystals were cut into the shape of cylinders with polished edges at 5 mm diameter. The behavior shown in these data sets, while not conclusive, is consistent with the results from SFM poling experiments. In Fig. 2, threshold behavior for the poling dynamic of congruent material is evident. Because of this observed behavior, fabricating large domain structures (or fabricating small domain structures on thicker crystals) is carried out by increasing the amount of time the bias field is applied to through the crystal, rather than increasing the bias voltage. So far, no clear upper threshold in domain size has been observed in changing the magnitude of the applied voltage. Increasing this quantity will generate larger domains, however, the size of those domains is not limited by the material.

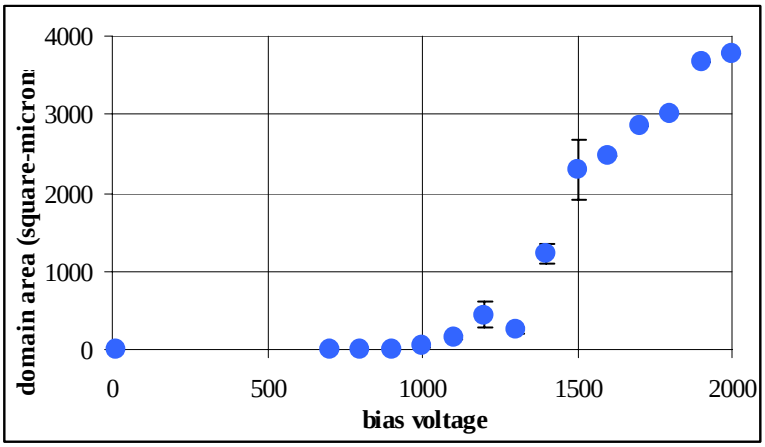

(a)

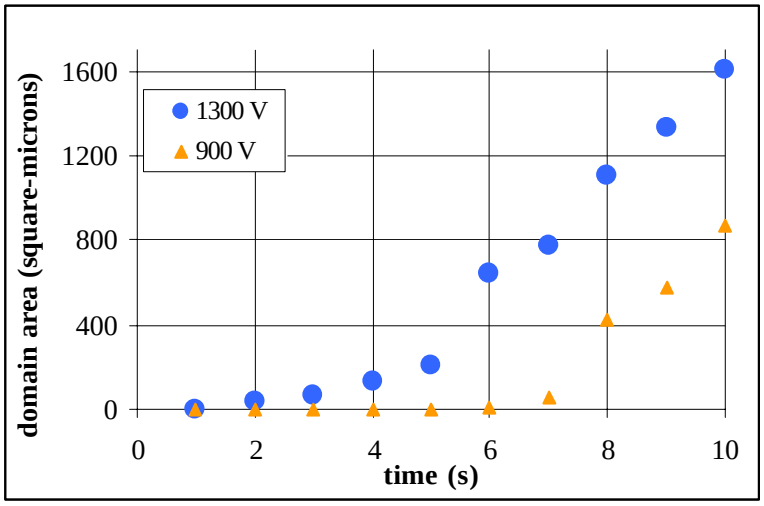

(b)

Fig. 3. Poling dynamics in 200 µm thick stoichiometric $LiNbO_3$. (a) Increasing bias voltage applied to different regions of the crystal for 5 s results in domain structures of increasing size. (b) Increasing the time a given bias voltage is applied will result in domains of increasing size.

An advantage of calligraphic poling is the option of erasing a poled structure on a crystal. We found some curious phenomena in the process. For example, Fig. 4 shows how the domain size depends on the poling history of the crystal. A domain was created in a 110 μm thick sample of congruent $LiNbO_3$ at some voltage applied for some time. The size of the domain was measured using the non-destructive visualization technique discussed in this article. The domain was then erased by inverting the sign of the applied field. After erasure, the same voltage was applied over the same amount of time to the same spot of the crystal. The size of the new domain was measured, and then it was erased again. This process was repeated for several iterations. The oscillations observed in the measured domain size in congruent samples could be attributed to a work-hardening analogue in ferroelectric domain reversal though we do not have explanation for the phenomenon. The nearly two orders of magnitude increase in the size of domains from the first iteration to the 12th iteration, and the subsequent stabilization of domain size in all subsequent iterations, shows that an intermediate step must be taken before $LiNbO_3$ (and possibly other ferroelectrics) is used as a high density memory storage device (such as the devices demonstrated in [17, 18]). For instance, before a thin crystal is put to use as a data storage device, the direction of polarization of the bulk crystal should be iteratively cycled several dozen times to ensure reliable writing and erasing of data.

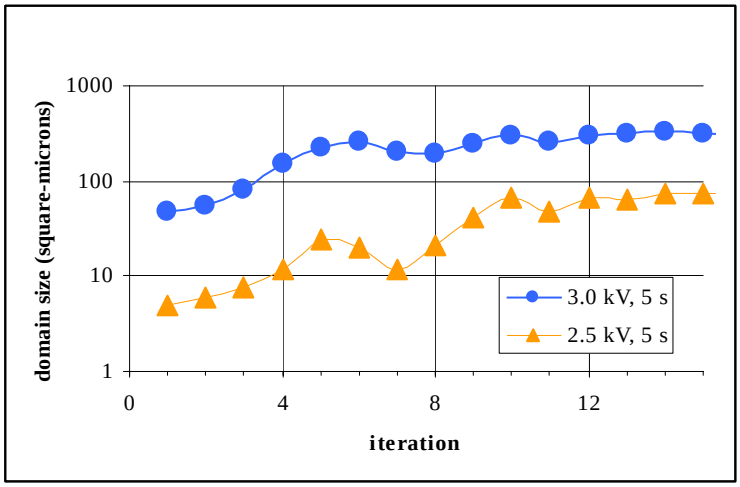

Fig. 4. Ferroelectric work-hardening in 120 μm thick congruent $LiNbO_3$. Domains are flipped, erased, and re-poled in successive iterations. The measured surface areas of the domains grow dramatically through several iterations.

3. Domain visualization

Visualization of the domains can be a part of the poling process. Light incident from above the crystal (+z-direction) reflects off of its bottom surface. As the voltage between the top and bottom surfaces in increased, the gradient in the refractive index of the narrow region between +z and –z poled regions increases. This results in distinct dark lines that outline regions of domain inversion, which are visible with the aid of an optical microscope. Note that unlike the conventional techniques that rely on polarization changes of light, polarizer/analyzer elements are not required for the visualization of the domains. Figure 5 shows the visualization of a ring-shaped domain structure applied via calligraphic poling techniques.

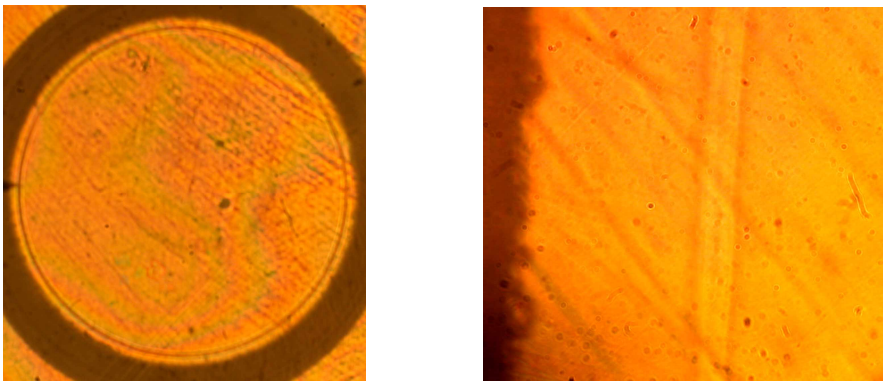

(a) (b)

Fig. 5. (a) A ring shaped poling pattern 2 μm edge to edge that follows the circumference of a disk shaped crystal. (b) Detail of a section of the ring. These images appear orange because of the brass substrate used as the bottom electrode.

Since domains are visualized as they are generated with the high voltage applied between the pen and the smooth substrate, calligraphic poling gives access to *in situ* monitoring of the domain growth process. Domain visualization occurs at far lower voltages than those required for domain reversal, however. The minimum voltage required to observe preexisting domain patterns, 200 V for 100 μm of thickness, is only a fraction of the voltage required to cause domain reversal to occur, thus the visualization technique is non-destructive. To verify that polarization flipping has taken place through the depth of the crystal, the crystal is flipped over and the same pattern is verified on the opposite side of the crystal. Figure 6 shows the visualization of hexagon-shaped domain structures achieved through calligraphic poling *ex situ* and *in situ*.

Since domain walls are regions of crystal that have a large gradient in the refractive index, the larger the bias voltage, the higher the resolution of domain wall boundaries. In Fig. 6(a), enough voltage was applied to make the domain walls of the hexagonally poled region visible. In Fig. 6(b), enough voltage is applied to cause domain reversal, which is more than enough for visualization of domains. To further increase visibility in Fig 6(b), the microscope is taken slightly out of focus, which allows for a primitive phase contrast imaging of the transparent domain structures. This is why the domain structures in Fig. 6(b) appear more distinct than the domain structure in Fig. 6(a).

As noted above, the bias field for domain reversal in stoichiometric material is much less than the required field for congruent material. Since domain reversal occurs at such smaller bias voltages in stoichiometric material, the field applied for visualization must be smaller. The result is reduced visibility of domains in stoichiometric material. As Fig. 6(a) shows, even this reduction in visibility still allows for observations of domain.

Applying a bias field is not the only way to visualize domains. For example, raising the temperature of a poled crystal allows for *ex situ* viewing of the domain walls through an optical microscope.

4. Poling near edges and other discontinuities

Poling near discontinuities require insulating oil because placing the pen, e.g., within 100 μm of the edge of the crystal causes at best no domain reversal, and at worse sparking that can result in the destruction of the crystal and the pen.

The steps for poling close to the crystal edges are the following. First, the crystal surface must be free of any scratches, cracks, or holes. This is visually verified by use of a microscope, and physically achieved by polishing or by any other means.

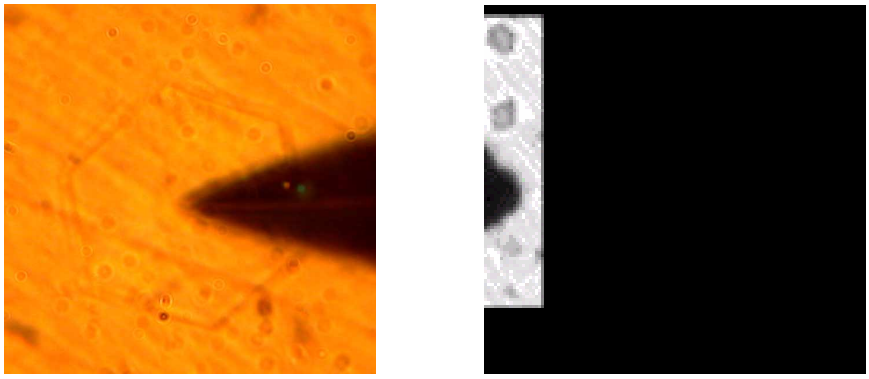

(a) (b)

Fig. 6. (a) A hexagonally shaped domain pattern in stoichiometric $LiNbO_3$ 24 µm edge to edge visualized ex situ. The large black arrow is the shadow of the pen used for writing and visualizing the domain. The sample was 110 µm thick with a radius of 6 mm. (b) A video of a linear chain of such hexagons written on congruent $LiNbO_3$ visualized in situ. This sample was 80 µm thick with a radius of 7.5 mm. (2.4 MB).

Second, the substrate in electrical contact with the lower surface of the crystal is polished to be cleared of all scratches. Any sharp points or discontinuities in its surface will cause an inordinate amount of charge to build up and result in a dramatic spark that can move or damage the crystal specimen. Using a metallic mirror as the substrate or polishing the substrate are simple ways to ensure a smooth substrate surface.

Once these steps are complete, a thin layer of saltwater is placed between the lower crystal surface and the smooth electrode. Over time, the weight of the crystal will squeeze out all but a thin film of the saltwater. This thin film will hold the crystal in place and keep out any other substance between the crystal and the lower substrate. Then, a hyrdrophobic insulating dielectric oil is added to cover the crystal and smooth electrode, as in Fig. 7. After enough time was given for all the excess salt water to leave the gap between the crystal and the substrate, the insulating oil surrounds the upper and edge surfaces of the crystal. The pen, which drags along the top surface of the crystal, causes charge to build up at its tip when a voltage is applied between the pen and the substrate. Since the crystal specimen is immersed in an insulating bath, the charge will continue to build up until an amount of charge sufficient for domain reversal is generated. Once this condition has been met, the permanent polarization of the region of the crystal immediately underneath the pen is reversed, causing a pulse of current to flow in the circuit.

The presence of the insulating oil does not affect the visualization of domains in any significant way. To see domain growth with a microscope, the image of the bottom surface of the crystal could be magnified. Thus, even as the shape of the drop of oil changes from bead-shaped to teardrop-shaped as the voltage is cycled on and off, the image of the bottom surface of the crystal does not change. Figure 8 is a demonstration of poling at the edge of a disk-shaped crystal immersed in oil.

Any oil or other material is cleared off from the calligraphic poling apparatus before the crystal is removed. Dousing the specimen in alcohol, then distilled water, and then acetone clears off most of the contaminants introduced in the calligraphic poling process. To remove the crystal, a single drop of salt water is placed near the edge. This drop will combine with the thin film of water underneath the crystal and cause a bead to form underneath the crystal, gently separating it from the substrate.

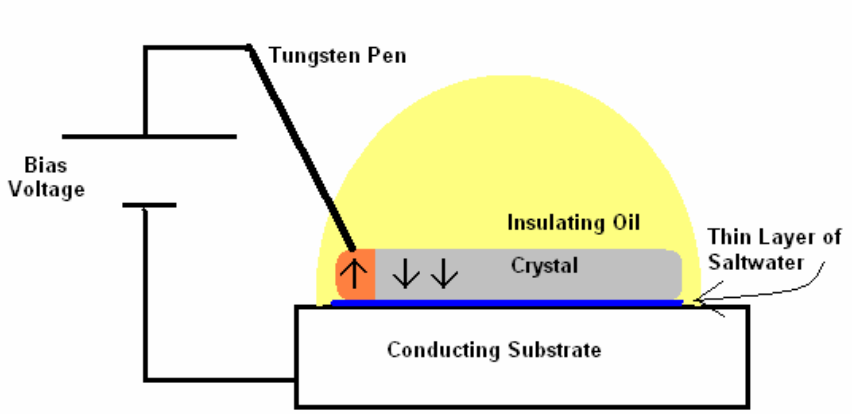

Fig. 7. Modification to the calligraphic poling machine to allow for edge-poling on a polished crystal. A hydrophobic, transparent, and insulating oil prevents sparks from charge build up on the edge of the crystal.

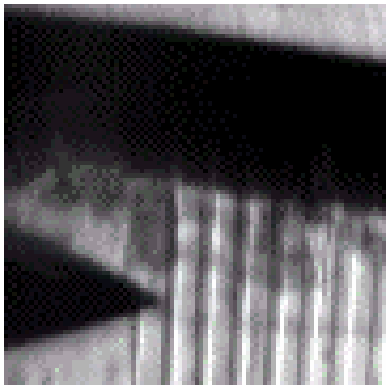

Fig. 8. Demonstration of poling at the edge of a disk shaped crystal with a diameter of 7 mm. Domains in the shape of radial lines 13 µm across (and 13 µm between) are draws with a 1 µm radius tungsten tip at 1.8 kV bias in real time. Two to three passes per line are made to ensure uniform domain thickness. Between stripes, the image goes out of focus because of the oil drop on top of the crystal (2.2 MB).

Another form of discontinuity is a scratch along the top surface of the crystal. When the charged pen is placed near a scratch, the charge density on the crystal surface will be largest in the area immediately underneath the tip of the pen, and the area along the scratch. This is because of the discontinuous sharp edges that define the scratch. In this scenario, we have observed domain growth along the scratch. The domains that were generated in this fashion were all of the hexagonal type. The thickness of the crystal should be uniform. However, using a mount that allows for the pen to rotate slightly, as described in section 2.1, reduces sensitivity to changes in thickness. The top surface can have up to 5 µm of variation in the thickness, while the bottom surface must be flat enough to ensure uniform electrical contact with the bottom conducting substrate.

5. Discussion

Calligraphic poling provides a versatile and cost effective way to generate complex domain engineered structures in ferroelectric crystals. By eliminating the requirements of other implementations (such as thermal control, vacuum systems, clean rooms, scanning force

microscopes and very high voltage dc sources) the average laboratory can now have direct access to experiments and to exploration of device engineering in quantum and nonlinear optics. Experimental groups focusing on ferroelectric devices could use calligraphic poling to generate prototypes of PPLN devices before purchasing preformed masks for mass production. Since the poling process occurs *in situ* and the visualization is possible in real time, the process of calligraphic poling is easy to monitor implement. The technique itself is also robust. One useful aspect of calligraphic poling is that a single crystal can be repeatedly poled with different patterns. That is, the poling pattern on a crystal can be erased (by reversing the voltage between the pen and the substrate) and a new one implemented either by hand or by computer control. Figure 9 shows an example of domain erasure.

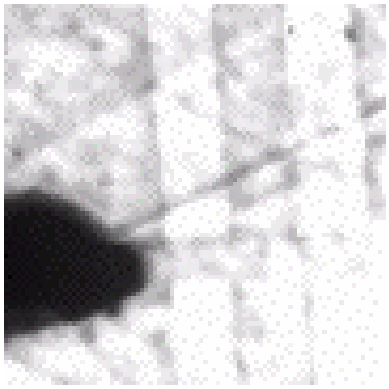

Fig. 9. Two linear domain structures 15 μm across are divided into sections by 'erasing' domain structures with the pen. The bias voltage between the pen and the substrate causes the previously +z poled regions to flip back to –z polarization (2.5 MB).

Calligraphic poling can be applied to optical whispering gallery (WGM) resonators to amplify nonlinear optical effects or to engineer device functionality. For example, periodically poled WGM resonators have been used as optical frequency doublers [12], as well as tunable optical filters [21] that can be utilized in high stability microwave sources. A calligraphically poled $LiNbO_3$ bulk crystal or waveguide could be placed within a Fabry-Perot or other type of optical cavity to achieve similar results.

Further experiments include generation of nonclassical states of light from periodically poled WGM resonators, and increasing efficiency of nonlinear optical processes in periodically poled WGM resonators.

6. Summary

Calligraphic poling is a low cost and easy to implement technique for domain engineering $LiNbO_3$. Calligraphic poling will be used as a tool to create high efficiency nonlinear optical and photonic bandgap devices. While lacking the potential for mass producing periodically poled nonlinear optical devices, as techniques using preformed masks have, calligraphic poling can be used to prototype such poling structures or to create unique poling geometries in-house at minimal cost. If the initial design fails, the poling structure can be erased and a new structure reapplied to the crystal.

Calligraphic poling can also be used as a tool to observe the real-time poling dynamics in crystals of varying aspect ratios under stress, under strain, and at various atmospheric conditions. The straightforward *in situ* visualization makes calligraphic poling particularly useful for this kind of experiment. The smallest domain structures visualized were on the order of μm^2. This is several orders of magnitude larger than the domain size generated through using a scanning force microscope, which can readily generate structures on the order of nm^2. While the larger resultant size of the domains (which may be made smaller by using a

narrower pen electrode) makes calligraphic poling a less desirable method for applications involving ferroelectric data storage, the real time visualization makes it a unique tool for measurements of crystal properties.

Finally, in addition to $LiNbO_3$, other z-cut 180º ferroelectric materials, e.g. $LiTaO_3$, can be domain engineered using calligraphic poling. z-cut MgO:$LiNbO_3$ [22] is another candidate for calligraphic poling that could lead to devices which are appealing for optics applications because of the reduced photorefractivity in such doped crystals. x-cut Crystals can also be poled using a variation of calligraphic poling.